

Supplementary Data

for

Oxidation-induced water-solubilization and chemical functionalization of fullerenes C_{60} , $Gd@C_{60}$ and $Gd@C_{82}$: atomistic insights into the formation mechanisms and structures of fullerenols synthesized via different methods

Part 1	S2
Part 2	S2
Part 3	S3
Part 4	S6
Part 5	S9
Part 6	S10
Part 7	S11
Part 8	S12

Part 1

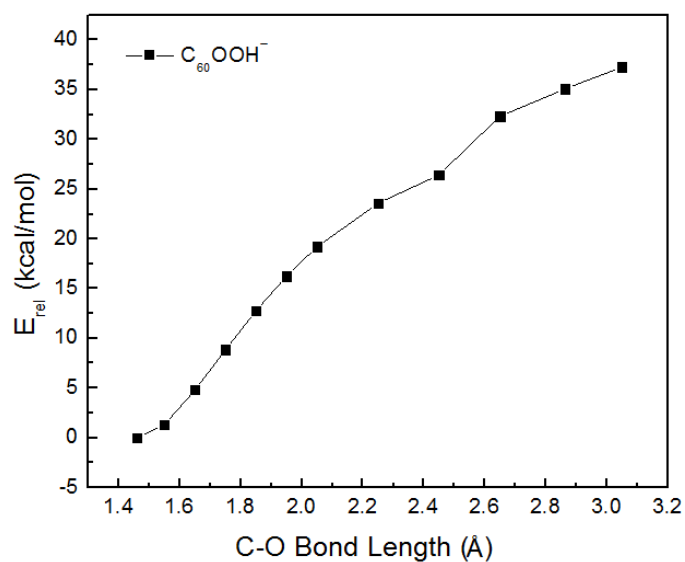


Figure S1. The energies of $C_{60}OOH^-$ with respect to the C-O bond length. Calculations were performed at B3LYP/6-31G(d,p) level of theory.

Part 2

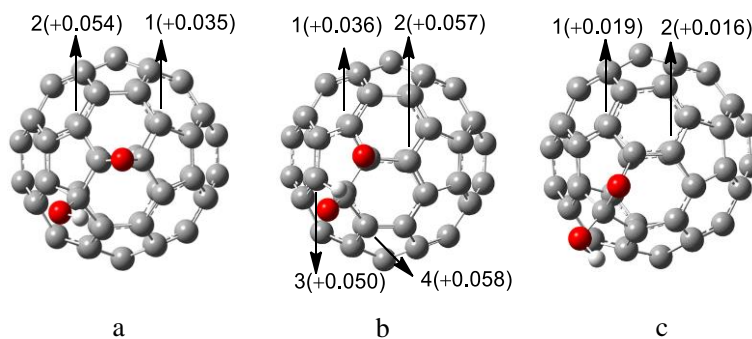


Figure S2. The Mulliken charge distributions for the most positively-charged positions of **int3-2** (a), **int3-4** (b) **int3-8** (c). Calculations were performed at B3LYP/6-31+G(d,p) level of theory.

Part 3

Table S1. Mulliken atomic charges of Gd@C₆₀. Calculations were performed at B3LYP/6-31+G(d,p) level of theory.

index of carbon	charges	index of carbon	charges	index of carbon	charges
40	0.09	51	0.00	18	-0.04
2	0.09	46	0.00	7	-0.05
10	0.05	14	0.00	39	-0.05
56	0.04	50	-0.01	12	-0.05
17	0.04	31	-0.01	26	-0.06
21	0.03	5	-0.01	16	-0.06
59	0.03	44	-0.01	28	-0.07
58	0.02	9	-0.01	38	-0.07
27	0.02	19	-0.01	43	-0.08
57	0.02	22	-0.01	25	-0.08
13	0.02	54	-0.01	45	-0.08
6	0.01	29	-0.01	35	-0.08
20	0.01	60	-0.01	37	-0.09
41	0.01	1	-0.02	53	-0.09
55	0.01	32	-0.02	15	-0.09
49	0.01	42	-0.03	47	-0.09
8	0.00	52	-0.03	11	-0.11
24	0.00	34	-0.03	30	-0.11
48	0.00	3	-0.03	23	-0.11
4	0.00	36	-0.04	33	-0.11

Table S2. Relative energies of $\text{Gd@C}_{60}\text{H}^-$ and $\text{Gd@C}_{60}\text{OH}^-$. Calculations were performed at B3LYP/3-21G-CEP-121G (E_{rel}^a) and B3LYP/6-31G-CEP-121G (E_{rel}^b and E_{rel}^c) level of theory.

Sub	$\text{Gd@C}_{60}\text{H}^-$	$\text{Gd@C}_{60}\text{H}^-$	$\text{Gd@C}_{60}\text{OH}^-$
index of	E_{rel}^a	E_{rel}^b	E_{rel}^c
carbon	(kcal/mol)	(kcal/mol)	(kcal/mol)
6	0.0000	0.066	0.000
17	0.0005	0.000	0.005
1	0.0007	0.006	0.006
13	0.0008	0.067	
2	0.0008		
9	0.0009		
11	0.0011		
15	0.0022		
35	0.0022		
4	0.0063		
25	0.0368		
12	4.2647	4.366	4.922
51	4.2648		
7	12.1515	11.419	11.556
49	12.1518		
3	12.1537		

According to Mulliken atomic charges of Gd@C_{60} (Table S1), we selected some species to calculate the energy of $\text{Gd@C}_{60}\text{H}^-$ by using B3LYP functional with 3-21G for nonmetal atoms and CEP-121G for Gd (Table S2). Next, basis sets B3LYP/6-31g(d,p) for nonmetal atoms and CEP-121G for Gd were used for the geometry optimizations of the 6 $\text{Gd@C}_{60}\text{H}^-$ species (Table S2). Finally, the 6 sites corresponding to the lower energy $\text{Gd@C}_{60}\text{H}^-$ were selected for the calculation of $\text{Gd@C}_{60}\text{OH}^-$. Basis sets B3LYP/6-31g(d,p) for nonmetal atoms and CEP-121G for Gd were used the optimizations of $\text{Gd@C}_{60}\text{OH}^-$.

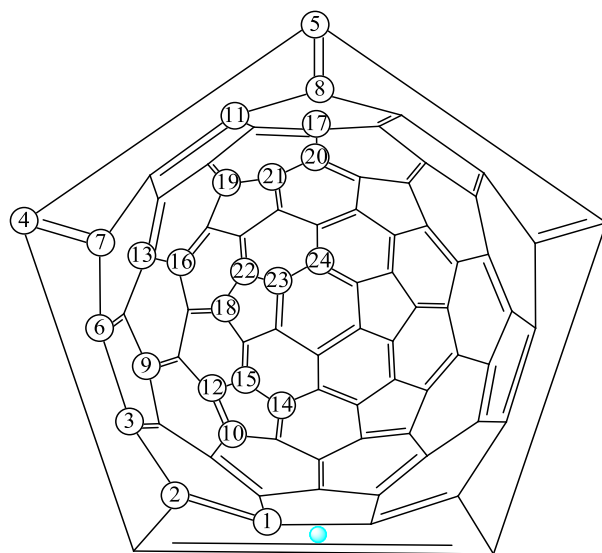


Figure S3. The 24 symmetrically unique addition sites of Gd@C₈₂.

Table S3. The relative energies of the 24 Gd@C₈₂OOH⁻ structures. Calculations were performed at B3LYP/3-21G-CEP-121G (E_{rel}^a) and B3LYP/6-31G-CEP-121G (E_{rel}^b) level of theory.

sites	E_{rel}^a (kcal/mol)	E_{rel}^b (kcal/mol)
2	0.00	0.00
7	5.15	4.56
23	6.51	5.76
8	9.27	8.45
18	9.60	8.45
13	9.69	7.90
21	10.08	
11	10.16	
4	10.54	
6	12.12	
14	12.55	
1	13.00	
12	13.64	
9	13.75	

10	14.59
5	14.93
19	14.93
22	16.92
15	17.56
16	20.61
17	20.80
24	24.42
20	26.37
3	28.55

For Gd@C₈₂, it has 24 symmetrically unique addition sites (Figure S3). First, we calculated energies of the 24 species Gd@C₈₂OOH⁻ using B3LYP functional with 3-21G for nonmetal atoms and CEP-121G for Gd (Table S3). Next, basis sets B3LYP/6-31g(d,p) for nonmetal atoms and CEP-121G for Gd were used for the optimization of the 6 lower-energy Gd@C₈₂OOH⁻ (Table S3).

Part 4

Table S4. Spin density distributions of Gd@C₆₀. Calculated with the B3LYP method in conjunction with 6-31+g(d) basis set for nonmetals and CEP-121G basis set for Gd atom.

index of carbon	spin densities	index of carbon	spin densities	index of carbon	spin densities
25	-0.11	46	-0.03	55	0.00
43	-0.11	31	-0.03	24	0.00
56	-0.09	50	-0.03	8	0.00
17	-0.09	26	-0.02	42	0.01
48	-0.08	16	-0.02	52	0.01
4	-0.08	13	-0.02	53	0.01
35	-0.07	57	-0.02	37	0.01
45	-0.07	7	-0.01	12	0.01

11	-0.05	39	-0.01	47	0.01
30	-0.05	10	-0.01	15	0.01
49	-0.04	5	-0.01	28	0.01
19	-0.04	44	-0.01	38	0.01
9	-0.04	33	0.00	54	0.01
32	-0.03	23	0.00	22	0.01
1	-0.03	51	0.00	6	0.02
36	-0.03	34	0.00	20	0.02
18	-0.03	3	0.00	27	0.02
29	-0.03	21	0.00	58	0.02
60	-0.03	59	0.00	2	0.02
14	-0.03	41	0.00	40	0.02

Carbon atoms 25, 17, 4, 11, 9 and 1 were selected to calculate the energy of Gd@C₆₀H·.

Table S5. Relative energies of Gd@C₆₀H· and Gd@C₆₀OH·. Calculations were performed at B3LYP/3-21G-CEP-121G (E_{rel}^a) and B3LYP/6-31G-CEP-121G (E_{rel}^b) level of theory.

sub	Gd@C ₆₀ H·	Gd@C ₆₀ OH·
index of	E_{rel}^a	E_{rel}^b
carbon	(kcal/mol)	(kcal/mol)
35	0.0000	0.007
17	0.0001	0.000
9	0.0002	0.007
11	0.0003	
4	0.0010	
1	0.0016	
25	0.0033	

According to the spin density distribution of Gd@C₆₀, it has 12 symmetrically unique carbon sites. (Table S4). Firstly, we selected the 7 most-negatively charged sites to calculate the energies of Gd@C₆₀H· by using B3LYP functional with 3-21G for nonmetal atoms and CEP-121G for Gd (Table

S5). Next, the 3 lower-energy species were selected for the calculation of Gd@C₆₀OH. Basis sets 6-31g(d,p) for nonmetal atoms and CEP-121G for Gd were used for the calculations.

Table S6. The relative energies of the 24 Gd@C₈₂OH. Calculations were performed at B3LYP/3-21G-CEP-121G (E_{rel}^a) and B3LYP/6-31G-CEP-121G (E_{rel}^b) level of theory.

sites	E_{rel}^a (kcal/mol)	E_{rel}^b (kcal/mol)
2	0.00	0.00
23	3.38	1.84
10	4.47	3.26
14	5.00	3.79
18	5.50	3.59
3	5.55	
4	6.51	
9	7.75	
19	8.34	
7	9.55	
11	9.65	
12	10.21	
6	13.89	
8	13.96	
13	14.26	
1	14.45	
21	14.64	
15	16.75	
5	17.73	
16	18.97	
22	20.31	
17	25.71	
20	30.91	
24	31.98	

For Gd@C₈₂, it has 24 symmetrically unique carbons (Figure S3). First, we calculated the energies for all these 24 Gd@C₈₂OH· structures using B3LYP functional with 3-21G for nonmetal atoms and CEP-121G for Gd (Table S6). Then, we selected 5 lower-energy structures to refine the energies using 6-31g(d,p) basis set for nonmetal atoms and CEP-121G for Gd (Table S6).

Part 5

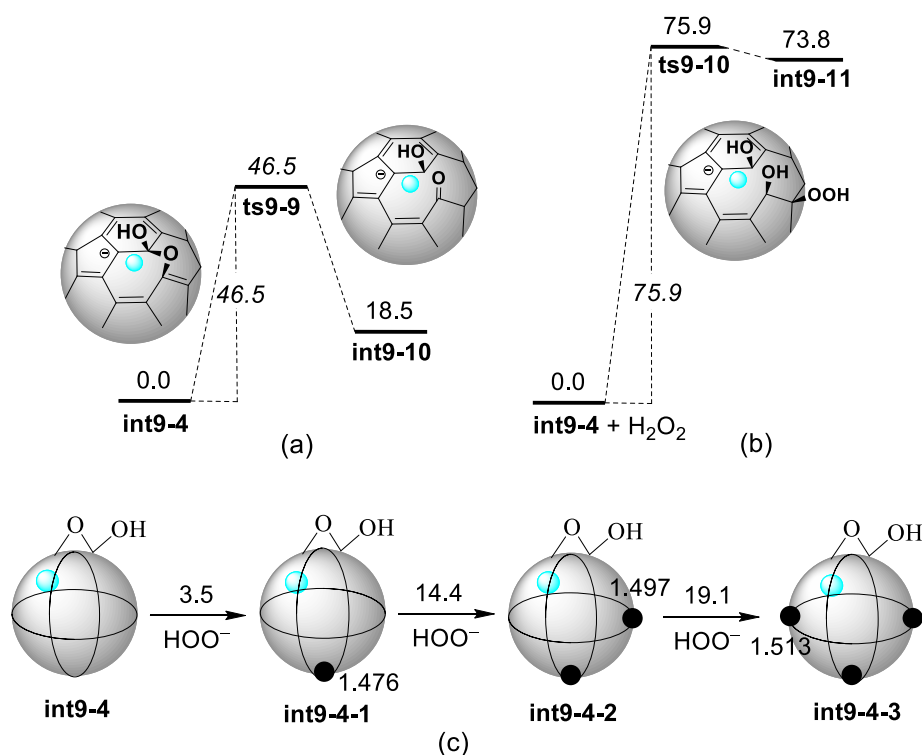


Figure S4. (a) The addition of H₂O₂ to **int9-4**. (b) Isomerization reaction for **int9-4**. (c) Consecutive additions of HOO⁻ to **int9-4**, in which change in Gibbs free energy (300 K, in kcal/mol) for each addition and the average C-O bond lengths (Å) of the corresponding adduct are marked. Filled circles in (c) represent the HOO⁻ groups. Calculations were performed at B3LYP/6-31G-CEP-121G level of theory.

An energy barrier of 46.5 and 75.9 kcal/mol indicate that the addition of H₂O₂ and isomerization to **int9-4** are difficult, respectively (Figure S4). Then, in order to determine whether or not the reaction could start at other sites of **int9-4**, HOO⁻ was chosen to be sequentially added to **int9-4**. The result

shows that the reaction energy and C-O bond lengthen gradually increase as the additions of HOO^- proceed. When the third HOO^- is added to Gd@C_{82} , the reaction energy becomes 19.1kcal/mol. This indicates that the third addition thermodynamically disfavored.

Part 6

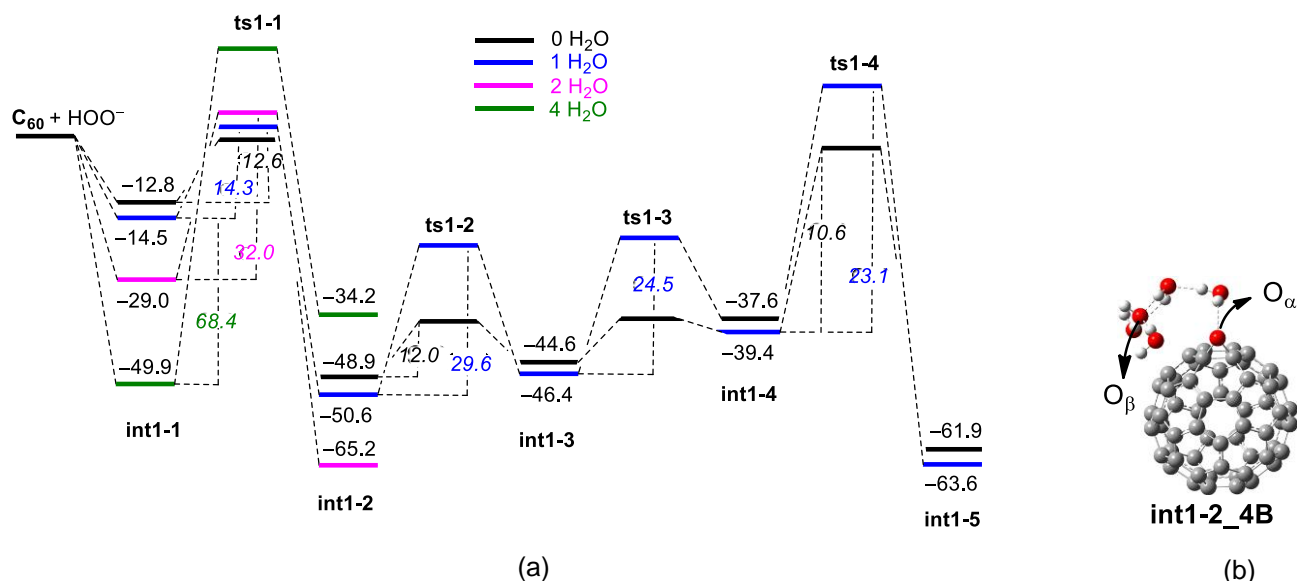


Figure S5. Reaction energy profiles for C_{60} epoxidation with the hydrogen peroxide anion, HOO^- . Up to four water molecules were considered as explicit solvent molecules. Shown in black, blue, pink and green lines are the paths in the presence of different numbers of water molecules. Values in normal and italic print typefaces depict relative Gibbs free energies (G_{rel} , in kcal/mol) and activation energy (kcal/mol), respectively, at 300K. Calculations were performed at B3LYP/6-31G-CEP-121G level of theory.

Figure S5 shows how explicit water molecules influence the hydroxylation of C_{60} with H_2O_2 in alkaline condition. The activation energies for the rate-determining steps increase from 12.6 kcal/mol (no water) to 29.6, 32.0, and 68.4 kcal/mol when one, two, and four water molecules are involved in the reactions, respectively. Therefore, water molecules will not directly participate into the reactions.

Part 7

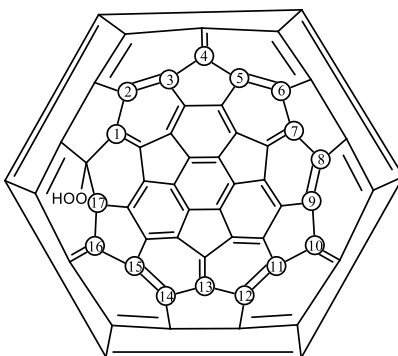


Figure S6. Skeletal structures for $C_{60}OOH^-$. Numbers depict the sites for the second HOO^- group.

Table S7. The relative energy of $C_{60}(OOH)_2^{2-}$. Calculations were performed at B3LYP/6-31G(d,p) level of theory.

sites	E (a.u.)	E_{rel} (kcal/mol)	sites	E (a.u.)	E_{rel} (kcal/mol)
9	-2588.1263	0.00	1	-2588.1199	4.06
2	-2588.1260	0.19	8	-2588.1191	4.53
17	-2588.1245	1.15	13	-2588.1188	4.71
5	-2588.1236	1.74	7	-2588.1182	5.11
14	-2588.1231	2.06	6	-2588.1154	6.87
3	-2588.1231	2.07	11	-2588.1146	7.40
15	-2588.1223	2.55	12	-2588.1140	7.77
4	-2588.1221	2.65	10	-2588.1089	10.95
16	-2588.1219	2.77			

Figure S6 depicts different addition positions of HOO^- to C_{60} . And their energies were calculated and presented in Table S7. Obviously, the addition in the site of 9 has the most lowest energy, which is considered the most stable addition position.

Part 8

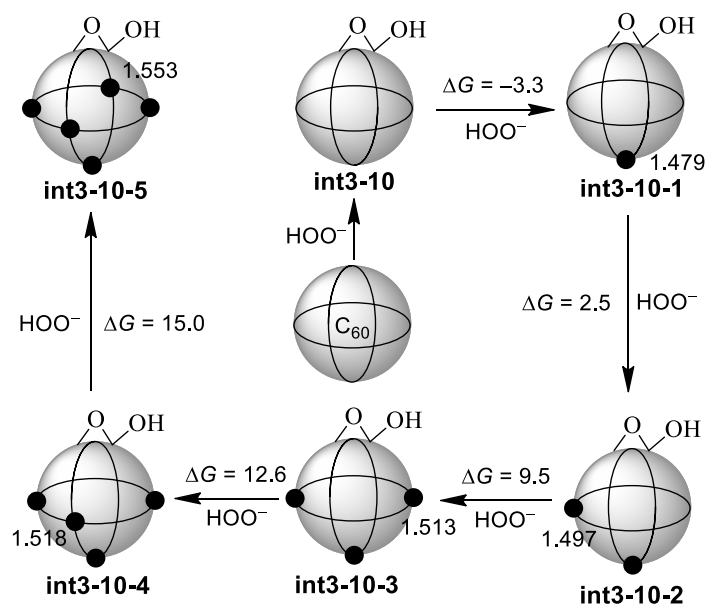


Figure S7. Consecutive additions of HOO^- to **int3-8**. Change in Gibbs free energy (300 K, in kcal/mol) for each addition and the average C-O bond lengths (Å) of the corresponding adduct are marked. Filled circles represent the HOO^- groups. Calculations were performed at B3LYP/6-31G-CEP-121G level of theory.

Figure S7 shows the average C-O bond lengths for the consecutive adducts of HOO^- to **int3-8**, which are 1.479, 1.497, 1.513, 1.518 and 1.553 Å, respectively. The increase of the bond length is consistent with the decreasing ΔG of these anions and increasing e-e repulsive energies. The tendency is analogous to that found for the reactions of HOO^- with C_{60} .